

Limiting effects in double EEX beamline

G Ha¹, J G Power², M Conde², D S Doran², and W Gai²

¹Pohang Accelerator Laboratory, Pohang, Gyeongbuk, 790-784, KOREA

²Argonne National Laboratory, Argonne, IL 60439, USA

E-mail: homehe@postech.ac.kr

Abstract. The double emittance exchange (EEX) beamline is suggested to overcome the large horizontal emittance and transverse jitter issues associated with the single EEX beamline while preserving its powerful phase-space manipulation capability. However, the double EEX beamline also has potential limitations due to coherent synchrotron radiation (CSR) and transverse jitter. The former limitation arises because double EEX uses twice as many bending magnets as single EEX which means stronger CSR effects degrading the beam quality. The latter limitation arises because a longitudinal jitter in front of the first EEX beamline is converted into a transverse jitter in the middle section (between the EEX beamlines) which can cause beam loss or beam degradation. In this paper, we numerically explore the effects of these two limitations on the emittance and beam transport.

1. Introduction

A program is underway at the Argonne Wakefield Accelerator (AWA) facility to develop an exchange-based method of longitudinal bunch shaping [1]. The current single emittance exchange (EEX) beamline is being upgraded to a double EEX beamline. After installation and commissioning is complete (in early 2018) it will first be used to study the capabilities and limitations of double EEX and, second, for applications requiring longitudinal bunch shaping. In this paper, we study the emittance growth from coherent synchrotron radiation (CSR) and jitter issues since they are expected to be the two biggest limitations of the double EEX beamline.

The first limitation we study arises from CSR which is an unavoidable side effect of all beamlines using dispersive elements (e.g. a dipole magnet). Since the EEX beamline uses multiple dipole magnets the beam has multiple chances to interact with CSR leading to emittance dilution. We note that the exchange process leads to a growth of the slice emittance in contrast to other dispersive beamlines (e.g. chicane) [2].

The second limitation we study is due to longitudinal jitter at the entrance to an EEX beamline that gets converted into the transverse jitter (i.e. horizontal offset) at the exit. This transverse jitter is critical because it can generate serious effects on the transverse optics and the emittance. Fortunately, since the double EEX beamline restores the phase space relationship, the converted transverse jitter after the first EEX becomes longitudinal jitters after the second EEX.

In this paper, we study these limiting issues in the AWA double EEX beamline using the particle tracking code GPT [3] with a CSR module [4]. The double EEX beamlines consists of two identical single EEX beamline and transverse manipulation section in the middle (See Figure 1). A double EEX beamline is simulated to study the jitter issue, but a single EEX beamline is used for the CSR study for the simplicity.



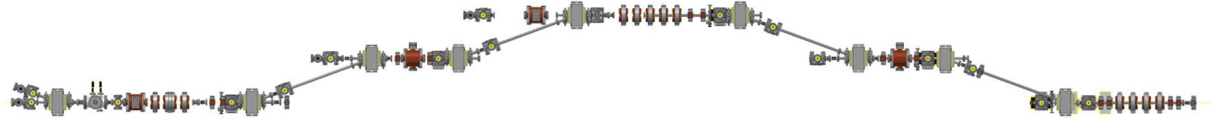


Figure 1. The schematic of a double EEX beamline. The beam is moving from the right to the left in this figure.

2. Emittance growth in the EEX beamline

The current AWA single EEX beamline [1] is used in the simulation study of emittance growth due to CSR. A 100 pC beam is numerically generated at the entrance to the double EEX beamline for the study. A horizontal emittance ($\varepsilon_{x,i}$) of this beam is $1 \mu\text{m}$. Bunch length (σ_z) and the chirp ($S_z \equiv \langle z\delta \rangle / \langle z^2 \rangle$) are varied around 2 mm and -2 m^{-1} respectively. The horizontal beam size (σ_x) and slope ($S_x \equiv \langle xx' \rangle / \langle x^2 \rangle$) are varied in 0.5–3 mm for the size and -1 m^{-1} to 1 m^{-1} for the slope.

The emittance growth without CSR is shown in Figure 2a as a function of the incoming beam parameters. The y-axis of this figure shows the ratio of the final longitudinal emittance ($\varepsilon_{z,f}$) to the initial horizontal emittance ($\varepsilon_{x,i}$) for the single EEX beamline. In this case, the 2nd-order or higher order terms are the only sources of the emittance growth. A smaller beam size normally generates a smaller emittance growth and an appropriate slope minimizes the high-order growth. Figure 2a follows the expected tendency. The horizontal slope near -0.2 m^{-1} suppresses this growth and a smaller transverse beam size induces a smaller emittance growth. The minimum emittance growth ($\varepsilon_{z,f}/\varepsilon_{x,i}$) is 1.05 with the initial beam size ($\sigma_{x,i}$) of 0.5 mm and the slope ($S_{x,i}$) of -0.2 m^{-1} .

The emittance growth with CSR is shown in Figure 2b as a function of the same incoming beam parameters as above. The overall patterns are similar to Figure 2a, since the higher order effects are dominant for this low charge, but the minimum emittance growths for each initial beam size increases due to CSR. This can be explained by Equation (1) which shows the emittance growth with the integrated momentum kick concept introduced in Ref. [5].

$$\Delta\varepsilon = \langle x_i^2 \rangle [\{\kappa L \Delta_z - (\eta + \kappa \xi L) \Delta_\delta\} S_x + \kappa (\Delta_z - \xi \Delta_\delta)]^2 + \frac{\varepsilon_{x,i}^2}{\langle x_i^2 \rangle} \{\kappa L \Delta_z - (\eta + \kappa \xi L) \Delta_\delta\}^2. \quad (1)$$

Figure 2c and d show the emittance growth plot for the bunch lengths of 1 mm and 0.6 mm respectively. A short incoming bunch length shortens the bunch length along the beamline. Due to the short bunch length, CSR along the beamline is stronger than the long bunch case (b). Since the higher-order effect competes with the CSR induced emittance growth (Equation (1)), the pattern and slope that minimizes the emittance growth change (Figure 2c and d). The optimal slope is 0 m^{-1} which yields a growth of 1.24 for $\sigma_z = 1 \text{ mm}$ case, and 0.2 m^{-1} provides 1.41 for $\sigma_z = 0.6 \text{ mm}$ case.

Figure 3 shows the emittance growth plot for different chirps. The top rows are the simulation results without CSR and the bottom is the results with CSR. Left column of the figure used the chirp of -2 m^{-1} and the right column used 0 m^{-1} while the bunch length is fixed to 2 mm for all cases. The emittance growth sources related to the longitudinal chirp are thick-lens effect [6] and CSR. The chirp of $-1/\xi$ minimizes the thick-lens effect but it also minimizes the bunch length in the middle of the EEX beamline (i.e. maximum CSR). Since the charge is low, the thick-lens effect looks stronger than CSR, so the chirp closer to $-1/\xi$ ($-1/\xi \approx -2 \text{ m}^{-1}$) reduces the emittance growth. Note, this trend depends on the charge level or the initial bunch length.

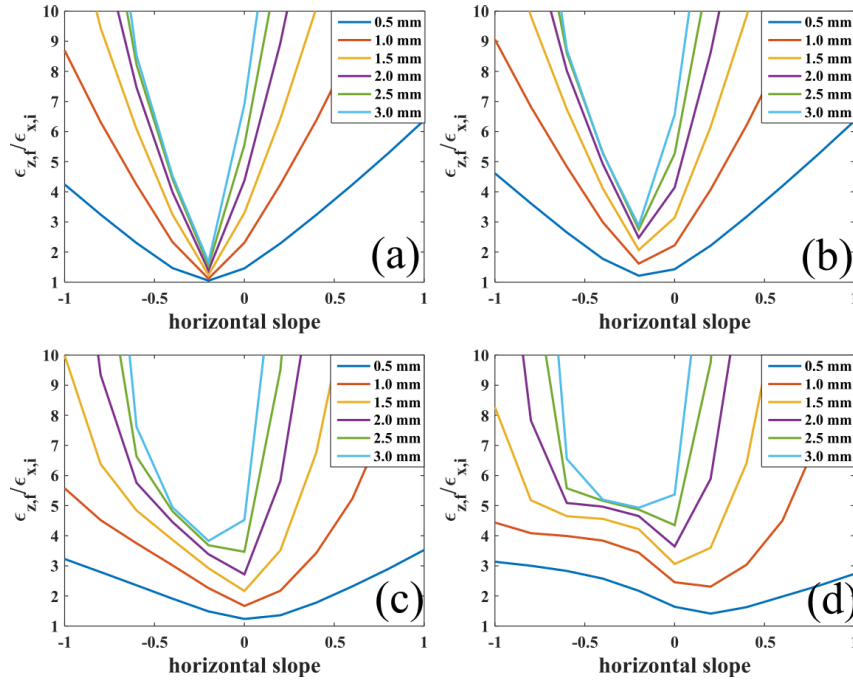


Figure 2. Emittance growth for various incoming beam parameters. The parameters $\varepsilon_{x,i} = 1 \mu\text{m}$ and $S_z = -2 \text{ m}^{-1}$ are fixed and the colors correspond to different values of σ_x . (a) $\sigma_z = 2 \text{ mm}$ (without CSR), (b) $\sigma_z = 2 \text{ mm}$ (with CSR), (c) $\sigma_z = 1 \text{ mm}$ (with CSR), and (d) $\sigma_z = 0.6 \text{ mm}$ (with CSR).

3. CSR suppression

Since CSR is one of the major issues in modern accelerators, CSR suppression for the bunch compressor has long been studied. However, the study on CSR for EEX is started very recently. Here we tried to simulate two well-known ideas as a start: CSR shielding and low bending angle.

Figure 4 shows the simulation comparison with and without a shielding effect. Figure 4a is the result without the shielding effect, and Figure 4b includes the shielding effect. The plate gap size of 2 cm is applied to the dipole magnet area while the 5 cm gap is applied to the remainder of the beamline. For the $\sigma_x = 0.5 \text{ mm}$ case, the minimum emittance growths are 1.22 without the shielding and 1.12 with the shielding. Although the shielding gap limits the transverse optics, it is very effective way to suppress the emittance growth from CSR.

We also tried to minimize the emittance growth even further using both a smaller gap for the shielding and a low bending angle for the EEX beamline. The bending angle is changed from 20° to 5° , and the drift length of the dogleg is changed from 2 m to 5 m to keep the dispersion in a reasonable level ($\eta_{\alpha=20^\circ} = 0.89 \text{ m}$ and $\eta_{\alpha=5^\circ} = 0.46 \text{ m}$). The shielding uses 2 cm gaps for the whole beamline.

Figure 5 shows the simulation results with a low bend angle EEX beamline. Figure 5a and b use different initial bunch lengths (0.3 mm and 2 mm, respectively). The higher order effect generates a similar pattern as in Figure 2c and d. However, the short bunch now provides a smaller emittance growth than the long bunch. Since CSR is weak in this low bend angle case, the thick-lens effect dominates and the long bunch has the larger emittance growth. The minimum emittance growth in Figure 5a is only 1.06. Note, the thick-lens effect can be eliminated by introducing a fundamental mode cavity [6].

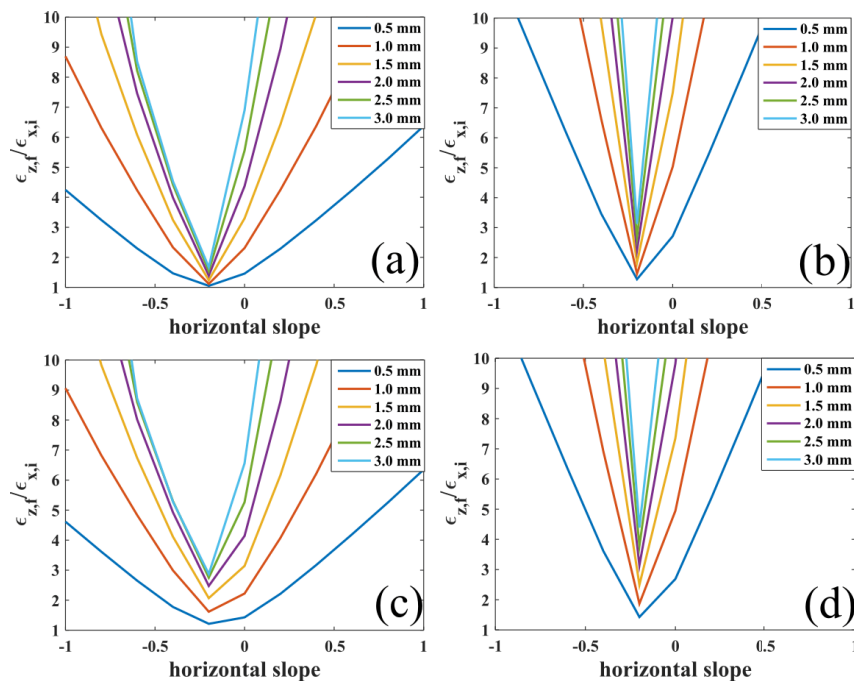


Figure 3. Emittance growth for various incoming beam parameters. Colors correspond to the initial beam size, and the initial emittance is $1 \mu\text{m}$. The top row are the simulation result without CSR and the bottom row are the result with CSR. The bunch length is fixed to 2 mm while the chirp is -2 m^{-1} for the left column and 0 m^{-1} for the right column.

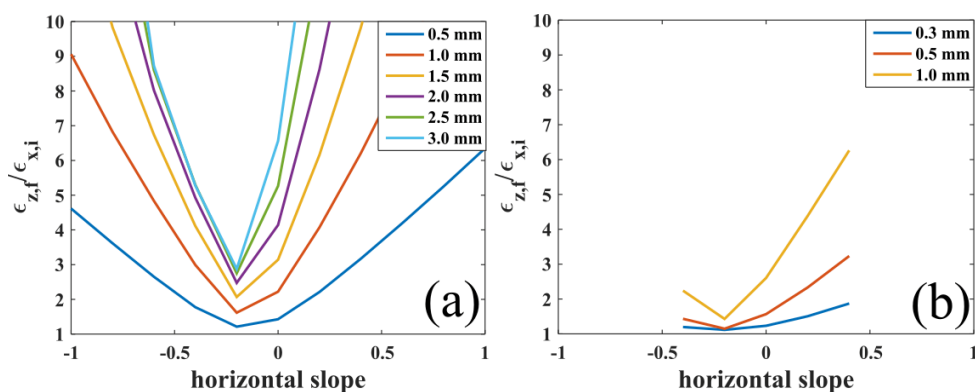


Figure 4. Emittance growth for various beam parameters (a) without CSR shielding and (b) with CSR shielding. Shielding gap is 2 cm for the dipole magnets and 5 cm for remainder. Initial emittance is $1 \mu\text{m}$, bunch length is 2 mm, and the chirp is -2 m^{-1} .

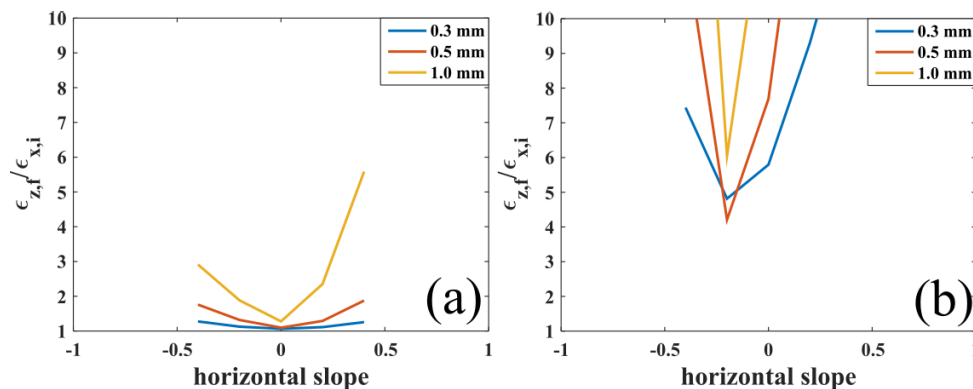


Figure 5. Emittance growth for various beam parameters with low angle EEX beamline. The dogleg parameters are changed to 5° bending and 5 m separation. Initial emittance of $1 \mu\text{m}$ and the chirp of -2 m^{-1} are fixed. The bunch length is (a) 0.3 mm and (b) 2 mm.

4. Longitudinal-to-transverse jitter conversion

As described earlier, any longitudinal jitter before the EEX beamline is converted to the horizontal jitter after a single EEX beamline due to the phase space exchange. In the double EEX beamline, however, the second EEX beamline brings all properties back to its original phase space, including jitter.

The jitter conversion along the double EEX beamline is shown in Figure 6a and b. For the artificially generated 100 pC beam, initial timing offsets are applied as a longitudinal jitter. When these beams arrive at the middle section (~ 8 m), the timing jitter is fully eliminated (See Figure 6b) and the beam has horizontal offsets (See Figure 6a). Once the beam passes the second EEX beamline, all horizontal offsets in the middle section disappear and the timing jitter appears again. Since the AWA-EEX beamline, with weak focusing, provides a little bunch compression, the final timing jitter is slightly reduced.

Figure 6c shows the emittance difference along the double EEX beamline due to timing jitter. At the end of the beamline, the largest emittance difference between the reference and the one with timing jitter is only $0.15 \mu\text{m}$ for -5 ps offset (initial emittance is $1 \mu\text{m}$). This emittance growth may come from the mismatch of the EEX condition in the second EEX beamline. (As a proof, even the transverse offset is not fully eliminated.) Another possibility is the emittance growth in the middle section. A large transverse offset in the middle section makes the beam pass the off-axis of the quadrupole magnets which introduce extra nonlinear fields. Even in this case, the emittance growth is reasonably small compared to the large timing offset, so it is not a major issue.

5. Summary and future work

We performed simulations to study the emittance growth due to CSR and the jitter conversion issue in the EEX beamline. We observed the trend of emittance growth originated from the higher order effect, thick-lens effect and CSR. We showed that the shielding method and the low bending angle suppress the emittance growth very effectively. The longitudinal jitter before EEX is converted to the horizontal offset in the middle section, and it is re-converted to longitudinal jitter by the second EEX beamline. During this process, the emittance is almost preserved and the jitter is slightly reduced.

Since this work was a simple scan-type simulation to study emittance growth and jitter issues, a theoretical study is required for further insight. We are also exploring the emittance growth

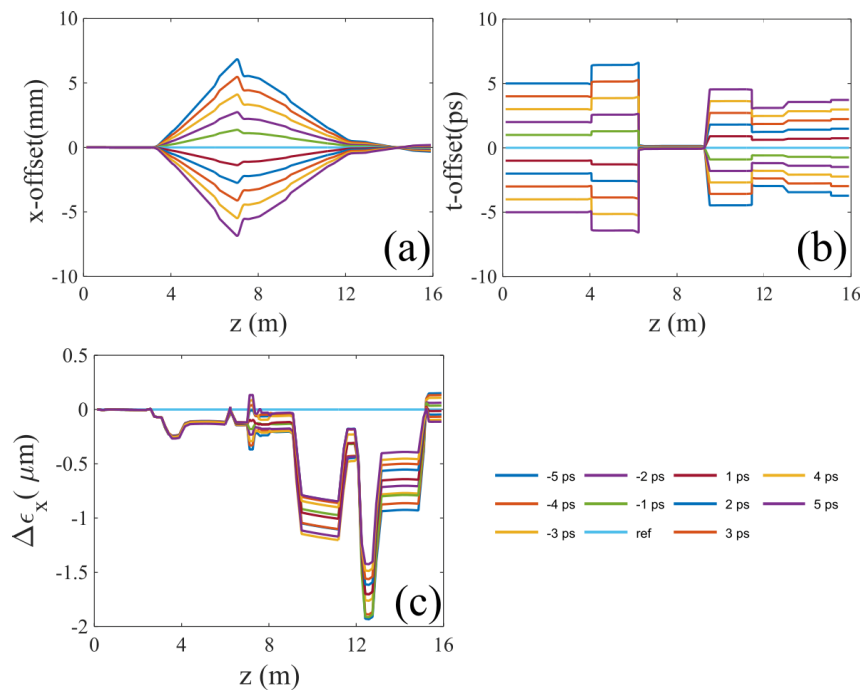


Figure 6. (a) Horizontal position, (b) timing, and (c) transverse emittance differences between the reference beam and the beam having initial timing offset. Simulation is done with 100 pC beam along the double EEX beamline. ~ 8 m is the middle section.

for high charge beam and trying to find other effective methods to suppress CSR.

Acknowledgement

This work is supported by Department of Energy, Office of Science, under Contract No. DE-AC02-06CH11357.

References

- [1] Ha G *et al.* 2017 *Phys. Rev. Lett.* **118** 104801
- [2] Guetg M W, Beutner B and Reiche S 2015 *Phys. Rev. Accel. Beams* **18** 030701
- [3] www.pulsar.nl/gpt
- [4] Bazarov I V and Miyajima T 2008 *Proc. European Partical Accelerator Conference 2008* (Mulhouse: EPS-AG) p 118
- [5] Ha G, Cho M H, Gai W, Kim K J, Namkung W and Power J G 2016 *Phys. Rev. Accel. Beams* **19** 121301
- [6] Zholents A and Zolotarev M S 2011 A new type of bunch compressor and seeding of a short wave length coherent radiation (*Preprint ANL-APS-LS-327*)